

# INTEGRATED PREDICTION TOOLS FOR WAVE OVERTOPPING AT VERTICAL STRUCTURES

Tom Bruce<sup>1</sup> and Jentsje van der Meer<sup>2</sup>

Overtopping prediction methods for steep and vertical structures are often presented as distinct sets of formulae for non-impulsive and impulsive conditions. Because these formulae use different non-dimensionalisation schemes, they are not simply plotted on the same axes. Thus, intuitive comparison and physical rationalisation of shifts between conditions has been difficult. This paper presents a reworking of prediction formulae from *EurOtop* (2007) which places formulae for non-impulsive and impulsive conditions on a more similar footing. The influence of a transition to impulsive conditions on mean discharge is now clear and physically-rationalised for plain vertical and composite vertical structures. Similarly, the influence of this transition (non-impulsive to impulsive) on the proportion of waves overtopping is also demonstrated on a single, easily-interpreted graph.

## INTRODUCTION

It is well established that wave overtopping discharge,  $q$  on many kinds of coastal structures generally decreases exponentially as the crest freeboard,  $R_c$  increases, with a form:

$$\frac{q}{\sqrt{g}H_{m0}^3} = a \exp\left(-b \frac{R_c}{H_{m0}}\right) \quad (1)$$

where  $H_{m0}$  is the spectral significant wave height, and  $a$  and  $b$  are fitting coefficients. For vertical breakwaters or seawalls, early work by Franco *et al.* (1994) gave  $a = 0.2$  and  $b = 4.3$ , while Allsop *et al.* (1995) gave  $a = 0.05$  and  $b = 2.78$ . *EurOtop* (2007) gives  $a = 0.04$  and  $b = 2.6$ .

There has however long been evidence that the overtopping process at vertical and steep walls cannot be described for all conditions simply by equations like Equation 1. Goda's design charts (*e.g.* Goda, 2000) show quite pronounced peaks for some shallower (relative) water depths. Physical model studies in the 1990s of overtopping at vertical walls under conditions where wave breaking on the structure was present, gave rise to new empirical fits of the form with a power law decrease in overtopping discharge with freeboard rather than an exponential one. Whether an equation of the form of Equation 1 or a power law should be used is determined by some discriminating parameter.

---

<sup>1</sup> School of Engineering, University of Edinburgh, King's Buildings, Edinburgh, EH9 3JL, United Kingdom Tom.Bruce@ed.ac.uk

<sup>2</sup> Van der Meer Consulting, P.O. Box 423, 8440 AK Heerenveen, The Netherlands. jm@vandermeerconsulting.nl

There is a great deal of evidence that these two, apparently distinct methods work well. The fact that discharge and freeboard are non-dimensionalised in quite different ways has however long prevented simple comparison of the formulae. Further, these differences prevent improved physical rationalisation of the transition from one regime to the other.

This paper presents a reformulation of the standard equations for impulsive overtopping at vertical walls (EA/Besley, 1999; *EurOtop*, 2007), which better integrates them into a more unified, physically rational framework of prediction tools.

### PLAIN VERTICAL WALLS

The starting point for the work are the equations given in *EurOtop* (2007), which are basically those given in the predecessor UK guidance (EA/Besley, 1999), adjusted to reflect the large amount of new data available since then and gathered in *CLASH*, see Steendam *et al.* (2004). The impulsive overtopping equations have the form of a power law:

$$\frac{q}{h_*^2 \sqrt{g h_s^3}} = a \left( h_* \frac{R_c}{H_{m0}} \right)^{-b} \quad (2)$$

where

$$h_* \equiv 1.3 \frac{h_s}{H_{m0}} \frac{2\pi}{g T_{m-1,0}^2} \quad (3)$$

$T_{m-1,0}$  is a spectral period ( $= m_{-1} / m_0$  – see *e.g.* *EurOtop*, 2007 for further explanation of, and justification for this period measure). The  $h_*$  parameter is used as a measure of “impulsiveness”, with a transition from non-impulsive to impulsive overtopping conditions at the wall taking place over the range  $0.2 \leq h_* \leq 0.3$ .

The coefficients  $a$  and  $b$  change depending on structure and wave conditions considered. The coefficient  $b$  in Chapter 7 of *EurOtop* (2007) takes values of 3.1 (for plain vertical walls, breaking waves), 2.7 (plain vertical, broken waves only) and 2.9 (composite vertical structures). These coefficients are simply the result of fitting to data – the differences have no basis in physical reasoning. But the fact that the coefficients are all different makes direct, *e.g.* graphical comparison between the different but closely-related structures and responses difficult. Coefficients  $b$  are all very close to 3 and none deviate far from the 2.92 of EA/Besley (1999). Allowing a “what if?” approach and fixing  $b = 3$  enables the equations to be algebraically manipulated:

Noting that Equation 3 can be written in a more physically-illuminating way:

$$h_* \approx 1.3 \frac{h_s}{H_{m0}} \frac{h_s}{L_{m-1,0}} \quad (4)$$

with  $L_{m-1,0}$  being the (fictitious) wavelength based on  $T_{m-1,0}$ . Equation 2 can now be rewritten as

$$\frac{q}{\sqrt{gh_s^3}} \frac{h_s^{3/2}}{H_{m0}^{3/2}} = a \frac{h_s^{3/2}}{H_{m0}^{3/2}} \frac{H_{m0}}{h_s} \frac{L_{m-1,0}}{h_s} \left( \frac{R_c}{H_{m0}} \right)^{-3} \quad (5)$$

$$\Rightarrow \frac{q}{\sqrt{gH_{m0}^3}} = a \sqrt{\frac{H_{m0}}{h_s}} \frac{1}{s_{m-1,0}} \left( \frac{R_c}{H_{m0}} \right)^{-3} \quad (6)$$

where  $s_{m-1,0}$  is the (fictitious) wave steepness with wavelength based on  $T_{m-1,0}$ .

Now we have the left hand side similar to Equation 1, the conventional way of showing dimensionless discharge. The equation is a power function of dimensionless freeboard  $R_c / H_{m0}$  instead of an exponential one. Equation 6 is much clearer than the formula with  $h_s$  on both sides (Equation 2). The form of Equation 6 is such that it can be seen that the overtopping under impulsive conditions depends on a combination of breaker index  $H_{m0} / h_s$  and the wave steepness  $s_{m-1,0}$ . Both breaker index and wave steepness have a physical meaning:

- $H_{m0} / h_s < \sim 0.4$ : waves are not depth-limited, but may be influenced by a gentle foreshore;
- $H_{m0} / h_s \sim 0.5$ : depth-limited conditions on gentle sloping foreshores (1:50 or gentler)
- $H_{m0} / h_s > \sim 0.6$ : depth-limited waves on steep foreshores
- $s_{m-1,0} = 0.06$ : wind waves near-maximum wave steepness (not reduced by depth-limited wave breaking)
- $s_{m-1,0} < \sim 0.02$ : low steepness, swell, or possibly due to wave breaking on a foreshore (which reduces the wave height, not the period).

Now, for the first time, predictions of a formula for impulsive conditions can be plotted directly alongside those for non-impulsive conditions on the familiar dimensionless discharge *vs.* dimensionless freeboard axes. To do this, a family of curves for impulsive conditions needs to be selected, with various combinations of breaker parameter and steepness. To do this, three indicative values of both breaker index ( $H_{m0} / h_s = 0.3$ ; 0.5 and 0.9) and steepness ( $s_{m-1,0} = 0.01$ ; 0.03 and 0.06) are used (Figure 1).

Figure 1 shows, as the straight line on the conventional overtopping axes, the formula given by *EurOtop* (2007) for non-impulsive conditions, with  $a = 0.04$  and  $b = 2.6$ . Also plotted, showing as curved lines, are Equation 6 with the combinations of breaker index and steepness listed above. The lowest lines (steep waves at deep water) coincide more or less with the non-impulsive lines, which is what we expect. Heavy breaking on a very steep foreshore gives the highest lines.

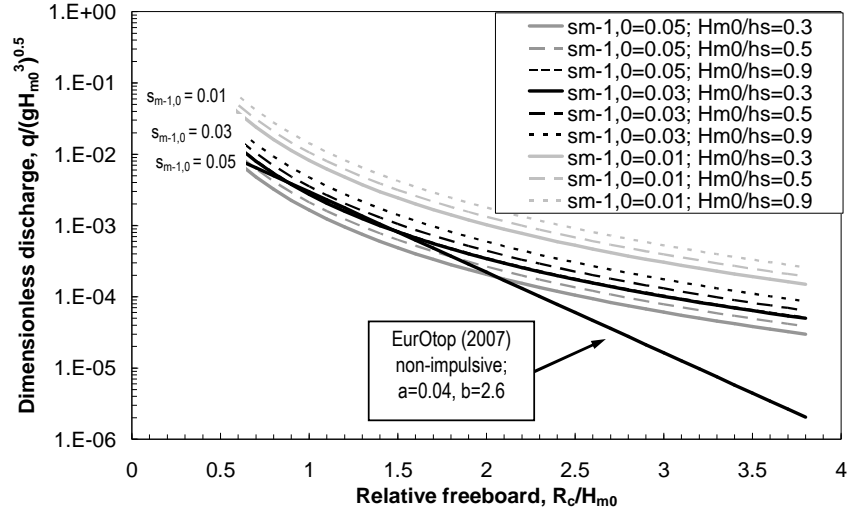


**Figure 1. Graphs for impulsive and non-impulsive formulae plotted on conventional axes. Note that the lines for ( $s_{m-1,0} = 0.05$ ,  $H_{m0} / h_s = 0.9$ ) and ( $s_{m-1,0} = 0.03$ ,  $H_{m0} / h_s = 0.3$ ) are coincident.**

Inspection of Equation 6 shows that, by including the breaker index and steepness in the vertical axis, all data for impulsive overtopping should come together. Data from all simple, plain vertical walls in the *CLASH* database is plotted with this new, adjusted y-axis,  $\{q / (gH_{m0}^3)^{0.5}\} / \{(H_{m0} / h_s)^{0.5} / s_{m-1,0}\}$  (Figure 2). Data with very low overtopping ( $q < 10^{-5}$  l/s/m) are excluded, as are those data classified in the *CLASH* database as being in the “not reliable” group (being assigned “reliability factor”,  $RF = 4$  and/or complexity factor  $CF = 4$ ) – see Steendam *et al.* (2004).

Figure 2 includes data that would be identified as “non-impulsive” by the  $h_*$  discriminator (Equation 3) suggested by *EurOtop* (2007), after EA/Besley (1999), and which therefore would not be expected to be fitted well by Equation 6.

Note that the  $h_*$  parameter and the new parameter  $(H_{m0} / h_s)^{0.5} / s_{m-1,0}$  are somewhat similar, both depending on breaker index and wave steepness:

$$\text{new transition parameter} = \left( \frac{H_{m0}}{h_s} \right)^{0.5} \frac{1}{s_{m-1,0}} = h_* \times \left( \frac{H_{m0}}{h_s} \right)^{-1.5} \quad (7)$$

Whether the new parameter would offer a useful discriminator for applicability of Equation 6 is explored. Plotting the effectiveness of the new scheme (Equation 6) as a ratio of measured:predicted discharges for all *CLASH* plain vertical wall data (Figure 3) shows that scatter is greatest for values  $(H_{m0} / h_s)^{0.5} / s_{m-1,0} < 20$ . As before, data with very low overtopping ( $q < 10^{-5}$  l/s/m) and  $RF = 4$  and/or  $CF = 4$  are excluded.

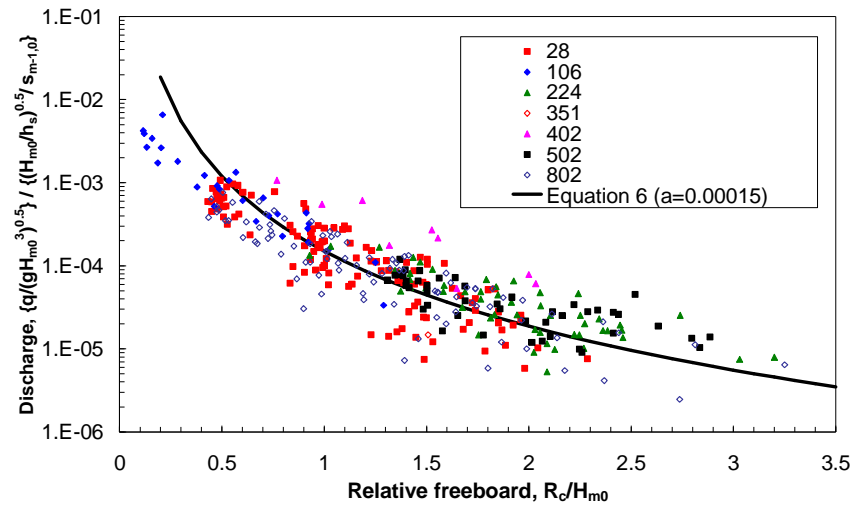


Figure 2. *CLASH* database plain vertical wall data with Equation 6 (note adjusted y-axis). Legend refers to data groups in *CLASH*.

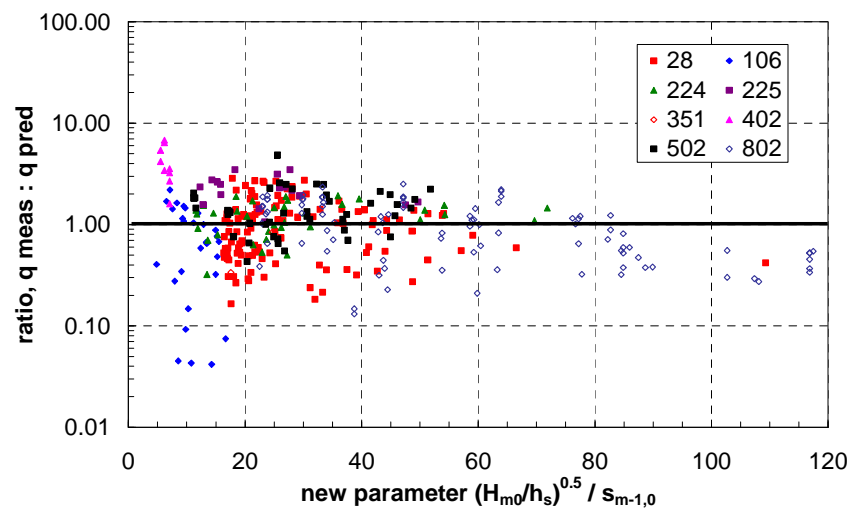
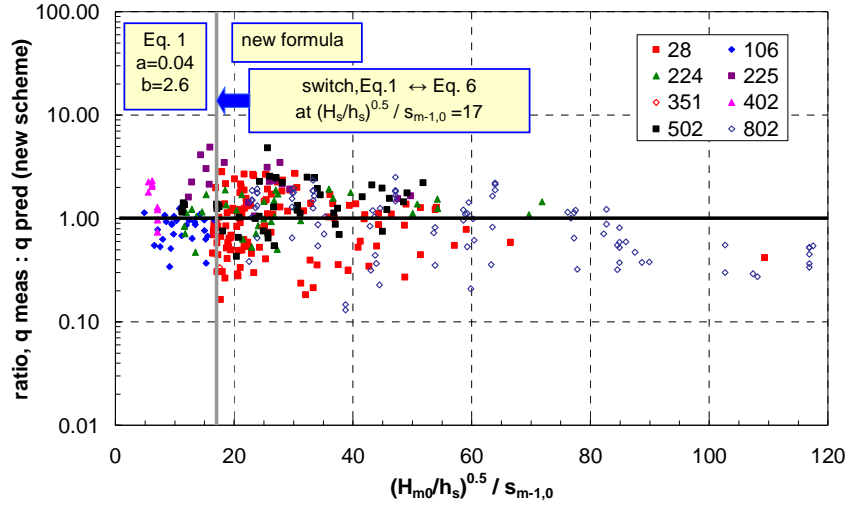


Figure 3. Ratio, measured:predicted discharges for *CLASH* database plain vertical wall data compared with Equation 6 (with  $a = 0.00015$ ). The large scatter for smaller values of the new parameter  $(H_{m0}/h_s)^{0.5} / s_{m-1,0}$  indicates non-impulsive conditions.

More detailed analysis shows that using  $(H_{m0}/h_s)^{0.5} / s_{m-1,0} = 17$  gives the best cut-off between data fitted best with the new formula (Equation 6) and the remaining data identified as “non-impulsive” and better fitted by an exponential form (*e.g.*) the non-impulsive form suggested by *EurOtop* (2007) – Equation 1

with  $a=0.04$ ,  $b=2.6$ . The resulting method, combining Equation 1 for non-impulsive conditions and Equation 6 for impulsive, and with the new transition parameter sees all data and predictions agreeing to within a factor of 10, and is generally a little conservative (Figure 4).



**Figure 4.** Ratio, measured:predicted discharges for *CLASH* database plain vertical wall data compared with result of new method for data with  $(H_{m0}/h_s)^{0.5}/s_{m-1,0} > 17$ .

The effect of the changes from the *EurOtop* (2007) method, *viz* the fixing of the power in Equation 2 to  $b=3$ , and the incorporation of the new impulsive / non-impulsive discriminating parameter  $(H_{m0}/h_s)^{0.5}/s_{m-1,0} = 17$ , is quantified using a log-based measure of the error in which factor of (*e.g.*) 3 over-prediction contributes the same to the summed error as a factor of 3 under-prediction:

$$\varepsilon = \log_{10} \frac{q_{\text{measured}}}{q_{\text{predicted}}} \quad (8)$$

Thus, on Figures 3 and 4,  $\varepsilon$  is essentially a measure of the distance of a point away from the perfect agreement line at ratio = 1. The mean value of  $\varepsilon$  will give a measure of the overall success of the prediction scheme against *CLASH* database data. The results, excluding data with  $q < 10^{-5}$  m<sup>3</sup>/s/m and those data classified in the least reliable group ( $RF = 4$  and/or  $CF = 4$ ), are summarised in Table 1. From this, it is clear that the new scheme is at least as effective as *EurOtop* (2007), with 68% of predictions lying within a range of  $\times/\div 2.2$ . As per *EurOtop*, it also errs very slightly on the (safe) side of over-prediction.

Table 1. Comparison of success of new prediction scheme with <i>EurOtop</i> (2007).		
	mean error $\bar{\varepsilon}$ (Equation 8)	standard deviation in $\bar{\varepsilon}$ , $\sigma_{\bar{\varepsilon}}$
new scheme	- 0.018	0.338
<i>EurOtop</i> (2007)	- 0.024	0.307

### COMPOSITE VERTICAL WALLS

For impulsive conditions at composite vertical structures, *EurOtop* (2007) gives

$$\frac{q}{d_*^2 \sqrt{gh_s^3}} = 4.1 \times 10^{-4} \left( d_* \frac{R_c}{H_{m0}} \right)^{-2.9} \quad (9)$$

where

$$d_* \equiv 1.3 \frac{d}{H_{m0}} \frac{2\pi h_s}{gT_{m-1,0}^2} \quad (10)$$

with  $d$  being the water depth above the berm. In the same way that the  $h_*$  parameter (Equation 3) is used in the *EurOtop* (2007) method as a discriminator between impulsive and non-impulsive conditions at a plain vertical wall, so  $d_*$  discriminates between two sets of formulae for composite vertical structures. In almost the same way as for Equation 4, Equation 10 for  $d_*$  can be written in a form which offers some sense of its physical origin:

$$d_* \approx 1.35 \frac{d}{H_{m0}} \frac{h_s}{L_{m-1,0}} \quad (11)$$

As for composite vertical walls, it is not straightforwardly possible to analyse in a generic way the differences between impulsive and non-impulsive forms, and even harder to get a sense of the physical transition.

Following the algebraic approach used (above) for plain vertical walls, setting the power index in Equation 10 to 3, Equation 12 is arrived at:

$$\frac{q}{\sqrt{gH_{m0}^3}} = b \sqrt{\frac{H_{m0}}{h_s}} \sqrt{\frac{d}{h_s}} \frac{1}{s_{m-1,0}} \left( \frac{R_c}{H_{m0}} \right)^{-3} \quad (12)$$

It is immediately clear that this is a much more physically-rational equation – the apparently separate formulations for plain and composite vertical structures have been reduced to a single set, with the difference between Equations 6 and 12 being a simple factor of  $(d/h_s)^{0.5}$  which becomes unity for plain vertical walls with zero berm height ( $h_s = d$ ) and which offers the potential for a physical rationalisation of the influence of the berm level. With the power of  $(R_c/H_{m0})$  only changing from 2.9 (Equation 9) to 3 (Equation 12), the effect on the predictor's success is lost in the “noise”. Further work needs to be done,

however, to examine the most appropriate choice of the discriminating parameter which allows selection between impulsive form (Equation 12) and the form for non-impulsive conditions (of the form of Equation 1).

Also, the constant multiplier ( $b$ ) in Equation 12 is not the same as that for plain vertical walls (Equation 6), so some further work needs to be done, focussed on the influence of small mounds, to truly combine Equations 6 and 12 into a single predictor.

### INDIVIDUAL OVERTOPPING VOLUMES

As for mean discharge, existing guidance offers different formulae for the statistical distribution of overtopping volumes associated with individual wave events (and implicitly therefore, different formulae for the estimation of the maximum individual overtopping volume,  $V_{\max}$ ).

The number of overtopping waves is important to make the distribution of individual overtopping volumes. For non-impulsive wave overtopping, the equation for the number of overtopping waves became a Rayleigh distribution:

$$\frac{N_{ow}}{N_w} = \exp\left\{-\left(\frac{1}{0.91} \frac{R_c}{H_{m0}}\right)^2\right\} \quad (13)$$

For impulsive overtopping waves, *EurOtop* (2007) gives

$$\frac{N_{ow}}{N_w} = 0.031 \frac{1}{h_*} \frac{R_c}{H_{m0}} \quad (14)$$

In order to bring together the Equations 13 and 14 so that some physical insight can be gained, a relationship with  $R_c/H_{m0} \times h_*$  was found for impulsive waves which was then re-fitted to a Weibull function (Equation 15).

$$\frac{N_{ow}}{N_w} = \exp\left\{-\left(13.5 h_* \frac{R_c}{H_{m0}}\right)^{0.58}\right\} \quad (15)$$

Note that a Weibull function includes a Rayleigh distribution ( $b=2$  as in Equation 13), and an exponential distribution for  $b=1$ . Equation 15 has even a lower  $b$ -value than an exponential distribution, which means that it is a very steep distribution.

Both formulae (Equations 13 and 15) are shown in Figure 5, with  $R_c/H_{m0}$  as horizontal axis, and with lines for various  $h_*$ . The way in which individual maximum volumes for impulsive conditions “lift off” from the non-impulsive line for higher  $R_c/H_{m0}$  can be identified clearly, as can the fact that small  $h_*$  give more overtopping waves.



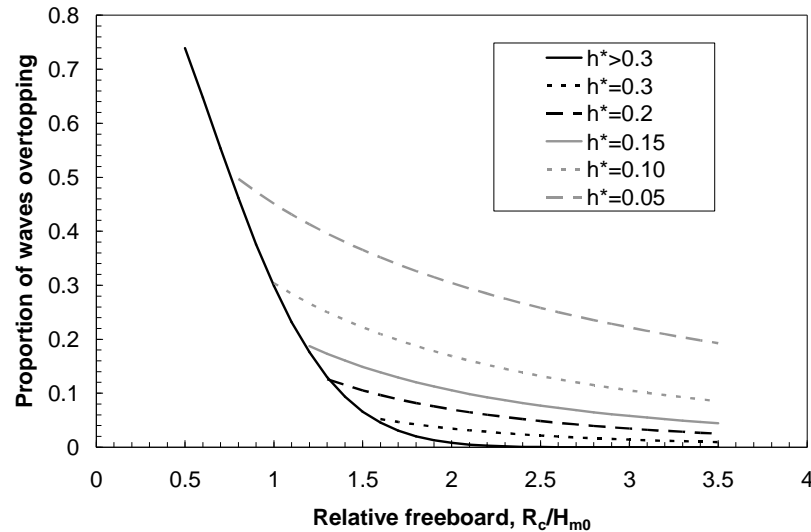


Figure 5. Proportion of waves overtopping; non-impulsive and impulsive conditions, showing effect of “impulsiveness parameter”,  $h$ . (Equation 3). Solid line ( $h > 0.3$ ) represents non-impulsive conditions; lower  $h$  conditions are increasingly-strongly impulsive.

## CONCLUSIONS

1. Previously separate / distinct sets of prediction formulae for overtopping at vertical walls have been brought together, both for mean discharges and individual volumes, allowing formulae for both impulsive and non-impulsive conditions to be plotted on the same axes.
2. New physical insight has been gained into transitions between overtopping responses, both in terms of mean discharge and individual volumes, to non-impulsive and impulsive wave attack at the primary wall.
3. Rational, simple modifications to plain wall formulae are offered for composite structures (instead of further, apparently different formulae).

## ACKNOWLEDGMENTS

The authors are grateful to *EurOtop* colleagues William Allsop, Andreas Kortenhaus, Tim Pullen and Holger Schüttrumpf for useful discussions.

Tom Bruce acknowledges the support of the Scottish Funding Council for the Joint Research Institute with the Heriot-Watt University, a part of the Edinburgh Research Partnership.

**REFERENCES**

- Allsop, N.W.H., Besley, P. & Madurini, L. 1995. Overtopping performance of vertical walls and composite breakwaters, seawalls and low reflection alternatives. Final report of *Monolithic Coastal Structures (MCS)* project, University of Hannover
- EA / Besley, P. 1999. *Overtopping of seawalls – design and assessment manual*, R & D Technical Report W 178, Environment Agency, Bristol, ISBN 1 85705 069 X
- EurOtop. 2007. *European Manual for the Assessment of Wave Overtopping*, Eds. Pullen, T., Allsop, N.W.H., Bruce, T., Kortenhaus, A., Schüttrumpf, H. & van der Meer, J.W., [www.overtopping-manual.com](http://www.overtopping-manual.com)
- Franco, L., de Gerloni, M. & van der Meer, J.W. 1994. Wave overtopping on vertical and composite breakwaters. *Proc. 24th Intl. Conf. on Coastal Eng.*, 1030–1045, ASCE
- Goda, Y. 2000. *Random seas and design of maritime structures (2nd edition)*, World Scientific Publishing, Singapore, ISBN 981-02-3256-X
- Steendam, G-J., van der Meer, J.W., Verhaeghe, H., Besley, P., Franco, L. & van Gent, M.R.A. 2004, The international database on wave overtopping, *Proc. 29th Intl. Conf. on Coastal Eng.*, 4301–4313, ASCE / World Scientific, Singapore, ISBN 981-256-298-2

KEYWORDS – ICCE 2008

PAPER TITLE **Integrated Prediction Tools for Wave Overtopping at Vertical Structures**

Authors **Dr Tom Bruce and Dr Jentsje van der Meer**

Abstract number **356**

Breakwaters

Coastal structures

Overtopping